Synthesis of New Ceramics from Powder Mixtures Using Thermal Plasma Processing

Osamu Fukumasa

Department of Electrical and Electronic Engineering,
Faculty of Engineering, Yamaguchi University,
Tokiwadai 2-16-1, Ube 755-8611, Japan

Abstract

The synthesis of thermoelectric materials (β"-alumina) for the alkali metal thermoelectric converter (AMTEC) has been studied using a newly designed plasma jet reactor. Under not only atmospheric pressure but also low pressure, thin films of β"-alumina are successfully synthesized for the first time from powder mixtures of α-Al_2O_3, Na_2CO_3 and MgO. The powder-mixing ratio, jet power and substrate position strongly affect the synthesis of β" -alumina, which is found to be correlated with jet temperature. Synthesis of ferrite particles is also discussed. Under both atmospheric and lower pressures, ferrite particles are successfully synthesized from powder mixtures of Fe_2O_3, ZnO, NiO and CuO. In the high temperature region of the plasma jet, ferrite particles with high purity can be synthesized.

Key words: thermal plasma processing, plasma jet, synthesis of new ceramics, β"-alumina, ferrite particles

1. Introduction

Thermal plasma processing using a plasma jet with high speed and high heat capacity under reduced pressure (≦100 Torr) is one of the most promising methods for synthesizing new materials. To this end, we have developed a thermal plasma reactor [1, 2] composed of a forced constricted type plasma jet generator with a feed ring, and confirmed that this reactor generates stable plasma jets with a high heat capacity under various operating conditions[1, 2]. So far, we have shown the performance of the reactor in the production of ultrafine particles and new ceramics [1-3] and spray coatings of refractory materials [4], as well as in the synthesis of diamonds [5, 6]. The typical deposition rate of spray coating with this system is approximately 5μm/s and that of diamond films is 5 - 6 μm/min. These deposition rates are higher than those of other methods by two or three orders of magnitude.

In this paper, rapid syntheses of β"-alumina and ferrite particles from powder mixtures are studied. For β"-alumina synthesis [3, 6], we will discuss the relationship between the temperature of the plasma jet and the synthesis of β"-alumina films. For synthesis of ferrite particles, we present some preliminary data and discuss dependences on processing conditions.

The alkali metal thermoelectric converter (AMTEC), which utilizes sodium ions which conduct β"-alumina solid electrolyte, is a device that directly converts heat energy to electric energy [7, 8]. In general, it is necessary to reduce the thickness of the β"-alumina layer to improve the generating power densities. According to our recent experimental results [4], the characteristics of thin films prepared by plasma spraying depends strongly on the operating pressure and dense films without pores are obtained under low pressure. We expect that β"-alumina would be synthesized from powder mixtures and dense and thin β"-alumina coatings would be prepared successively by low-pressure plasma spraying. However, a porous molybdenum electrode is expected to be prepared under atmospheric pressure.

Ferrite carriers have been used for electrophotography as a developer mixture with toner to forming the magnetic brush and to develop the latent image on the photoconductor. Ferrite carriers are a spherical beads with mean particle size from 40 to 100μm and consist of the soft ferrite material of Ni-Zn or Cu-Zn etc.[9]. The desired characteristics for the ferrite

carrier is higher magnetization, certain range of electrical resistivity and chargeability in addition to the particle size and its distribution. For a color printer with fine electrophotographic processing, the particle size is expected to be from 10 to 20 μm [10]. Usually, ferrite carriers are prepared from powder mixtures by some complex processes (namely, presintering, milling, granulating and sintering). It takes approximately 10 hours to produce ferrite carrier from powder mixtures. Therefore, rapid process of producing fine ferrite carriers is well expected in the future.

2. Experimental Set Up

A schematic drawing of the plasma reactor system [1-6] used in the present work is shown in Fig.1. Details are described elsewhere [1, 2]. The system consists of the forced constricted type (FC-type) plasma jet generator (the nozzle anode made of copper with 5 mm diam., the insulated constrictor nozzle made of copper with 5 mm diam., and rod cathode made of 2%Th-W), the feed ring (FR) (5mm diam.) and the vacuum vessel (160 mm diam. by 500 mm length).

Experiments are performed under continuous pumping and flowing of argon gas. The plasma jet is produced by DC arc discharge. As the insulated constrictor nozzle peculiar to this generator always fixes the arc length and the nozzle wall strongly constricts the arc with working gas, the plasma jet is kept very stable and has high power under various experimental conditions [1, 2]. For β"-alumina synthesis [3, 6], powder mixtures ofα-Al_2O_3, Na_2CO_3 and MgO are injected into the plasma with carrier gas through two capillary feeding ports of the FR. However, raw materials of Fe_2O_3, ZnO, NiO and CuO are used for synthesis of ferrite particles.

Experiments are made under the following conditions: working gas (Ar) flow rate is 20 *l*/min., jet power (W_j) is 3 - 6 kW, pressure in reaction chamber (P_t) is 100 and 760 Torr, feed gas (Ar) flow rate is 6 *l*/min., powder feed rate is 0.5 g/min., and the distance from the feed ring exit to substrate (L) is 25 - 110 mm. Throughout this experiment, a molybdenum substrate is used and its size is 15 mm in diameter and 1mm in thickness.

3. Experimental Results and Discussion

3.1. Production and control of plasma jet

With the use of the floating constrictor nozzle, our newly designed reactor (i.e. FC-type generator) produces stable plasma jet for various operating conditions as the arc column is fixed at constant length [1, 2]. Besides these, thermal efficiency is kept at 65% - 75% and these values are larger than those of a conventional-type plasma jet generator (nozzle anode without floating constrictor nozzle).

Fig. 2 shows the photographs of the plasma jet at P_t = 760, 100 and 5 Torr. Under the low pressure of 5 Torr, the plasma jet expands and its diameter increases to about 50 mm. Namely, with decreasing P_t, plasma jet increases in its size of both the axial and radial directions. Corresponding to this, high temperature region and high velocity region expand. With increasing W_j, high temperature and high velocity regions further expand in the downstream region. Fig. 3 shows the axial distributions of the plasma jet temperature at two different pressures, P_t = 760 and 100 Torr. As is clearly shown, with increasing W_j or decreasing P_t, the high-temperature region shifts to the downstream region.

According to these results, we can control parameters of the plasma jet (velocity, temperature, volume) by varying P_t and W_j. In order to realize the large area deposition, we have studied the effect of P_t on diamond synthesis [5, 6]. In plasma spraying [4], injected particles should be fully melted and collided to the substrate with high speed. Therefore, by using plasma jet under low pressure, it is expected to obtain dense coating and to realize the plasma processing with high rate and large area deposition.

3.2. Synthesis of β"-alumina

The synthesis of β"-alumina was attempted using powder mixtures of α-Al_2O_3, Na_2CO_3 and MgO [11]. We have confirmed that β"-alumina is synthesized from powder mixtures of α-Al_2O_3, Na_2CO_3 and MgO, and there is an optimum percentage composition of MgO for synthesizing β"-alumina [3, 6, 11]. As far as we know, this synthesis of β"-alumina films is the first one prepared by thermal plasma processing, although β-alumina is included. Furthermore, there are some peaks of raw powder materials, i.e., peaks of α-Al_2O_3, Na_2CO_3 and MgO, in the X-ray diffraction patterns of the prepared films. To obtain a high thermoelectric conversion efficiency, pure β"-alumina films must be synthesized. For optimization of processing conditions, we discuss further the effects of W_j, P_t and L on the

synthesis of β"-alumina films.

Fig. 4 shows the X-ray diffraction patterns of the synthesized films as a function of L at P_t = 760 Torr. In the downstream region where L is greater than 40 mm, a small peak of β"-alumina is observed among the many peaks of the raw powder materials. On the other hand, in the upstream region where L is less than 30 mm, many β"-alumina peaks appear distinctly with decreasing L. At L = 25 mm, β"-alumina peaks become dominant, although small β-alumina and small MgO peaks are observed. Namely, pure β"-alumina films are well synthesized in the upstream region of the plasma jet, i.e., the high-temperature region of the plasma jet.

However, under low pressure (P_t = 100 Torr), we have also confirmed the same tendency that β"-alumina films are well synthesized with decreasing L. The optimum value of L is less than 50 mm. According to film analysis by EPMA, the ratio of Na to Al in the prepared films (at L = 50 mm) ranges from 1/4.7 to 1/6. This value is nearly the same as that of β"-alumina films prepared ideally, i.e. 1/5 - 1/7 [6].

Taking into account the results shown in Figs. 3 and 4 and the discussion described above, there should be a strong correlation between the jet temperature and the synthesis of β"-alumina films. Though the axial jet temperature is nonuniform at each gas pressure(i.e. 100 and 760 Torr), the temperature in the region where β"-alumina films are well synthesized is nearly the same regardless of P_t. Namely, the value is nearly equal to 2400℃.

Fig. 5 shows typical SEM images of the deposited film at L = 40 mm and 25 mm under P_t = 760 Torr. According to the X-ray diffraction patterns shown in Fig.4, β"-alumina is synthesized more successfully in Fig.5(b). The film in Fig.5(a) is composed of particles with diameter less than 10μm, which are not well melted, and the film is porous. On the other hand, the film in Fig.5(b) is dense as the deposited powders are well melted.

The melting points of Na_2CO_3 (852℃) and MgO (2800℃) are quite different. For β"-alumina synthesis, more sodium ions should be included in the prepared films than in β-alumina films. Therefore, at least MgO (i.e., the stabilizer of sodium ions) should be well melted in front of the substrate. Thus, β"-alumina is well synthesized in a high-temperature region (above 2400℃) of the plasma jet, and the optimum percentage composition of Na_2CO_3 also depends on the plasma jet temperature (or L and W_j)[3].

Fig. 6 shows X-ray diffraction patterns of the prepared films for three different conditions. With increasing W_j (see (a) and (b)), peaks of β"-alumina increase in their number and amplitude as jet temperature becomes high. With increasing the percentage of Na_2CO_3 (see (b) and (c)), peaks of β"-alumina increase markedly in their amplitude.

Effect of oxygen injection is also studied [12]. Oxygen injection enhances the synthesis of β"-alumina although optimum value of oxygen is not yet clarified.

Uniformity of the prepared films is pretty well although substrate size is small. As uniformity in thickness of the films is important and key point for application, this is discussed in the next step as a function of operating pressure.

The performance characteristics of the AMTEC strongly depend on two physical constants of the β"-alumina films, i.e., the thermal and electrical conductivities. In the preparation of β"-alumina, W_j , L and the percentage composition of powder mixtures have been found to be the key parameters, which are correlated with the plasma jet temperature and heat transfer from plasmas to particles. Optimization of the processing conditions where β"-alumina films with required physical constants are prepared is now under study.

3.3. Synthesis of ferrite

Fig. 7 shows photographs of the SEM images of prepared films on the molybdenum substrate with two different pressures, i.e. P_t = 760 and 100 Torr. X-ray diffraction patterns corresponding to the films in Fig.7 are shown in Figs.8 (c) and (d). For reference, patterns of raw powder mixtures (a) and commercial ferrite carriers (b) obtained by sintering are also presented. Patterns of both films, (c) and (d), obtained by plasma processing have the same peaks as the pattern (b). Thin films of ferrite are directly synthesized from powder mixtures of Fe_2O_3, ZnO, NiO and CuO not only under atmospheric pressure but also under low pressure.

The obtained samples are examined its magnetic property as a ferrite carrier. The magnetic properties are measured by vibrating sample magnetmeter (VSM). Most samples have sufficient magnetization value, i.e. above 60 emu/g although the magnetization depends on process conditions. By using EPMA and TEM, morphological observation and composition analysis of powders from prepared films are also carried out. Powders are spherical and composition is Zn-Ni-Cu ferrite.

To discuss the application feasibility for production of ferrite powders as carrier for electrophotography, synthesized powders are collected with ceramics saucer in the downstream region, i.e. L = 90 - 240 mm. Fig. 9 shows photographs of the SEM images of collected powders. According to the results of X-ray diffraction pattern, EPMA and TEM, we have confirmed that ferrite powders as a magnetic carrier are successfully synthesized although particle size is distributed.

Jet power W_j, L, P_t, processing duration time and injection of oxygen are also key parameters for ferrite synthesis, as described in discussion of β"-alumina synthesis. However, in synthesis of ferrite, the difference between melting point of powder mixtures is not so large as for that of β"-alumina although melting point is ranged from 1148℃(CuO) to 1998℃(NiO). So, rapid production of ferrite powder by thermal plasma processing should be well accomplished. Optimization of ferrite synthesis with high rate is now under study.

4. Conclusions

We have newly designed the thermal plasma reactor, where stable plasma jet with high thermal efficiency is produced for various operating conditions. With the use of this reactor, syntheses of β"-alumina films and ferrite particles are studied. Thin films of β"-alumina are successfully synthesized for the first time from powder mixtures of α-Al_2O_3, Na_2CO_3 and MgO not only under atmospheric pressure but also under low pressure. Ferrite films and ferrite powders are also synthesized from powder mixtures of Fe_2O_3, ZnO, NiO and CuO. The powder mixing ratio, jet power and substrate position strongly affect the syntheses of both β"-alumina and ferrite carriers, which is found to be correlated with jet temperature.

Acknowledgements

The author would like to thank S. Sakiyama, K. Fujioka (Toda Kogyo Corp.), J. Kim (Inha University, Korea), D. Mukunoki, M. Fujiwara and T. Tagashira for their collaboration of this work and for their support in preparation of the manuscript. A part of this work is supported by a Grant-in-Aid for University and Society Collaboration from The Japanese Ministry of Education, Science, Sports and Culture. This work is also supported by a Grant-in-Aid for Regional Consortium Project from New Energy and Industrial Technology Development

Organization (NEDO), Japan.

References

[1] O. Fukumasa and S. Sakiyama, Trans. IEE Jpn. **112A** (1992) 269. (in Japanese)

[2] S. Sakiyama, T. Hirabaru and O. Fukumasa, Rev. Sci. Instrum. **63** (1992) 2408.

[3] O. Fukumasa, S. Sakiyama and H. Esaki, Jpn. J. Appl. Phys. **38** (1999) 4571.

[4] O. Fukumasa, S. Sakiyama and K. Osaki, *Proc. The Japan-China Bilateral Symp. Advanced Materials Engineering* (1999), p.58.

[5] S. Sakiyama and O. Fukumasa, J. Jpn. Inst. Metals, **63** (1999) 55. (in Japanese)

[6] O. Fukumasa and S. Sakiyama, Surface & Coatings Technology, **131** (2000) 493.

[7] T. Cole: Science **221** (1983) 915.

[8] T. Masuda: Ceramics **25** (1990) 609. (in Japanese)

[9] H. Harada, T. Iimura and K. Eguchi, IEEE Tans. Mag. CHMT-9 (1986) 202.

[10] K. Fujioka, personal communication.

[11] O. Fukumasa, S. Sakiyama, Y. Shirai and K. Hatano, *Proc. 13th Symp. Plasma Processing*(1996), p.157.

[12] J. Kim, S. Sakiyama, O. Fukumasa and K. Osaki, *Proc. 17th Symp. Plasma Processing* (2000), p.463.

Figure Captions

Fig.1. Schematic diagram of the plasma jet reactor system.

Fig.2. Photographs of the plasma jet for three different pressures. Experimental conditions are as follows: Jet power W_j = 3 kW and working gas flow rate Q (Ar) = 20 l /min.

Fig.3. Axial distribution of the plasma jet temperature (determined from brightness temperature of W wire probe with using pyrometer) in the downstream region for two different pressures P_t = 100 and 760 Torr.

Fig.4. X-ray diffraction patterns of the thin films as a function of L. Symbols are β"(β"-alumina), β(β-alumina), ○(α-Al_2O_3), ▽(γ-Al_2O_3), △(Na_2CO_3), □(MgO) and ◇(Mo). Experimental conditions are as follows: W_j = 3 kW, P_t =760 Torr and powder mixtures are α-Al_2O_3 (68 %) + Na_2CO_3 (23 %) + MgO (9 %).

Fig.5. SEM images of the prepared thin films corresponding to the X-ray diffraction patterns in Fig.4, where L = 40 and 25 mm.

Fig.6. X-ray diffraction patterns of the prepared films for three different cases. Symbols are β" (β"-alumina), β(β-alumina), ○(α-Al_2O_3), ▽(γ-Al_2O_3). Experimental conditions are as follows: P_t = 760 Torr and L = 30 mm.

Fig.7. SEM images of the prepared thin films. Experimental conditions are as follows: W_j = 3 kW, L = 50 mm and deposition time T = 7 min.

Fig.8. X-ray diffraction patterns of raw powder mixtures, commercial ferrite powder (sintered) and two prepared films in the plasma. Symbols are F(ferrite), R1(Fe_2O_3), R2(ZnO), R3(NiO) and R4(CuO). The prepared films and process conditions are corresponding to those in Fig.7.

Fig.9. SEM images of the prepared powders. Experimental conditions are as follows: W_j = 3 kW, L = 120 mm and T = 10 min.

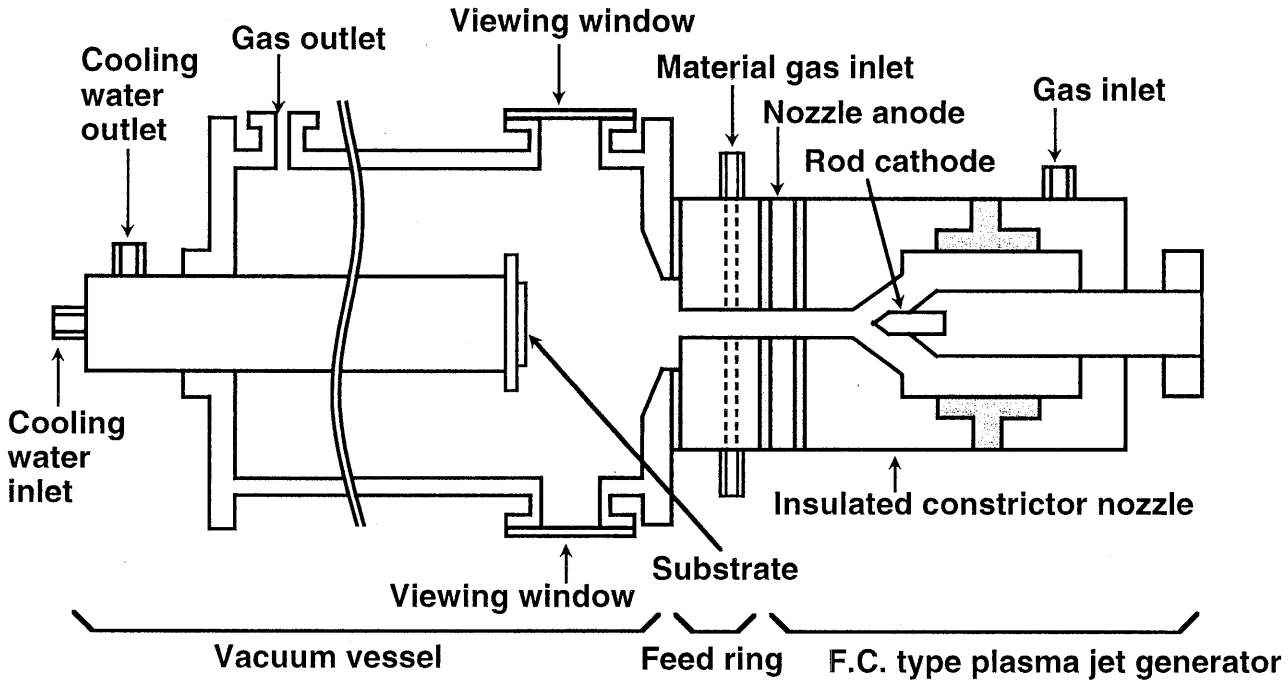

Fig.1 O. Fukumasa

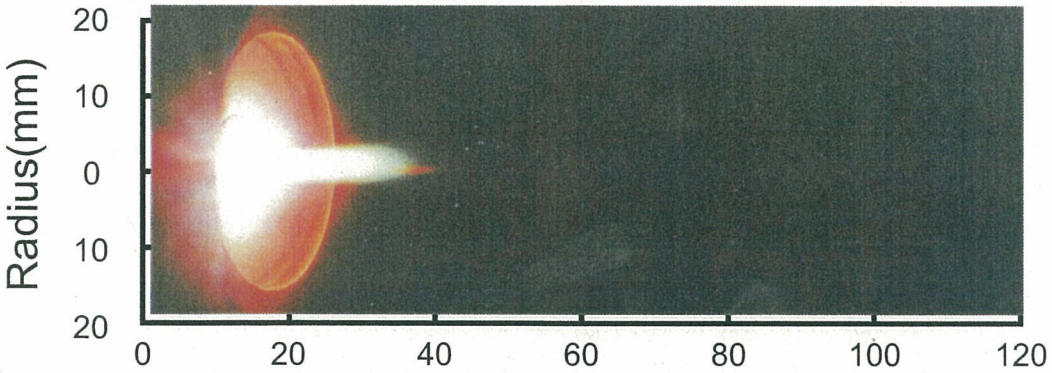

(a) Pt = 760 Torr

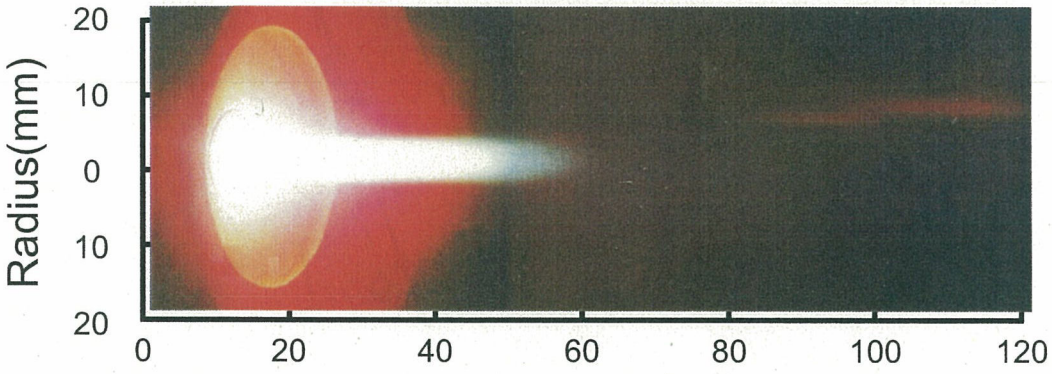

(b) Pt = 100 Torr

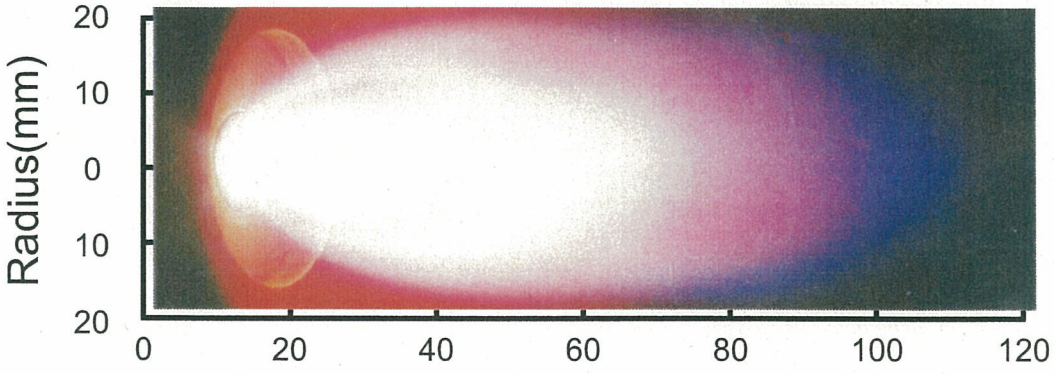

(c) Pt = 3 Torr

Fig. 2 O. Fukumasa

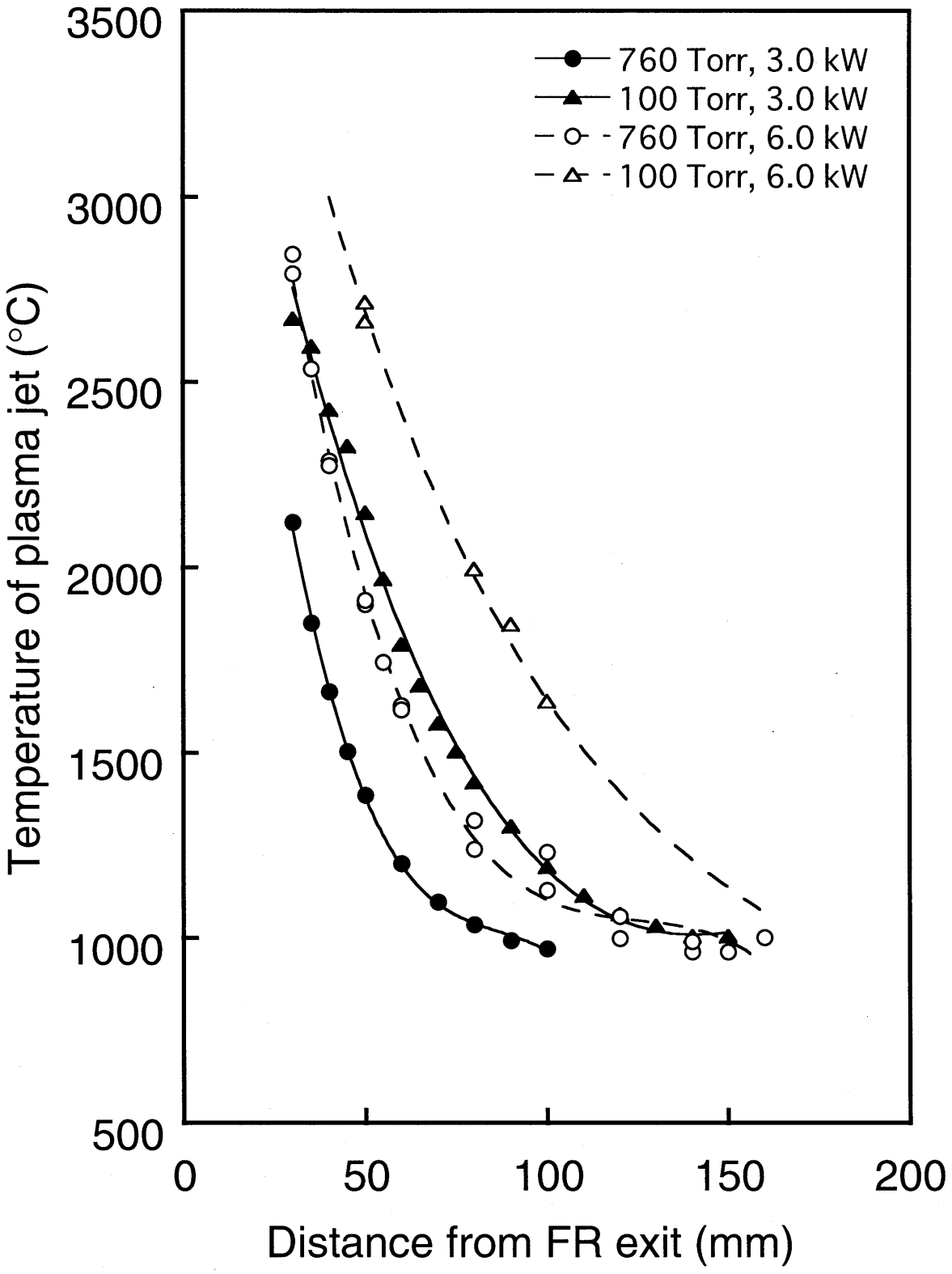

Fig. 3 O. Fukumasa

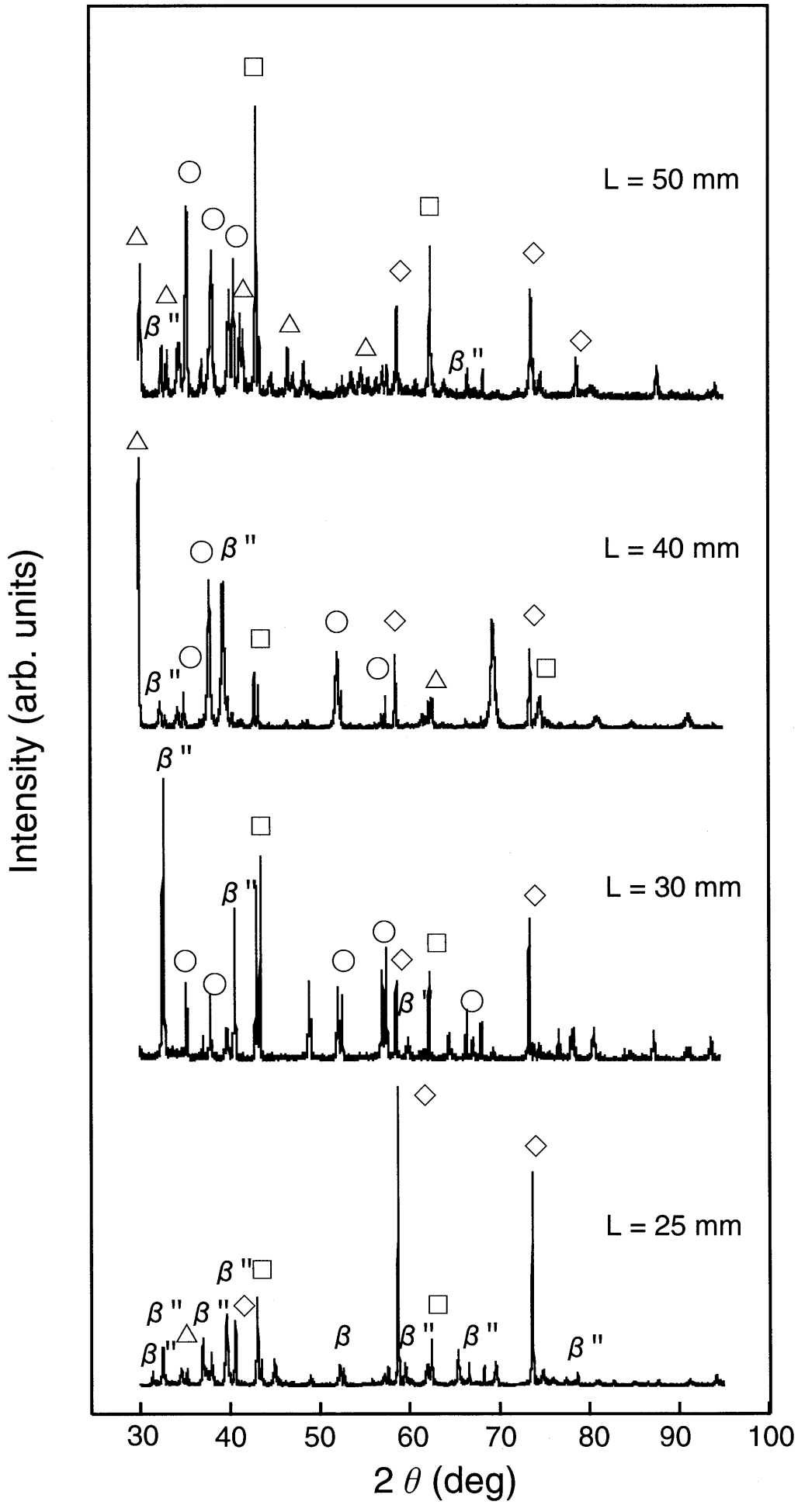

Fig. 4 O. Fukumasa

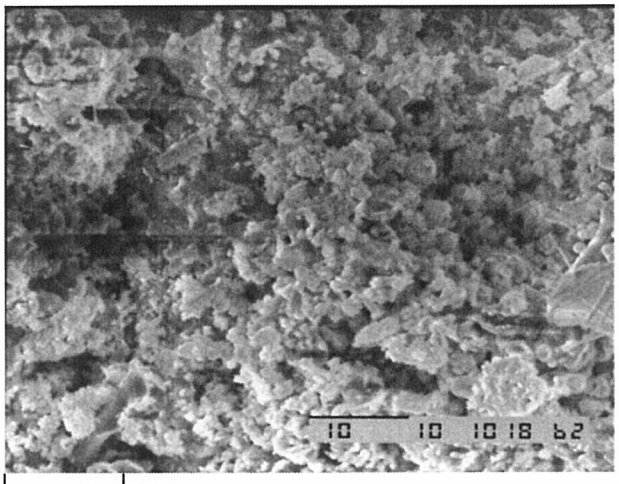

10 μm

(a) L=40mm

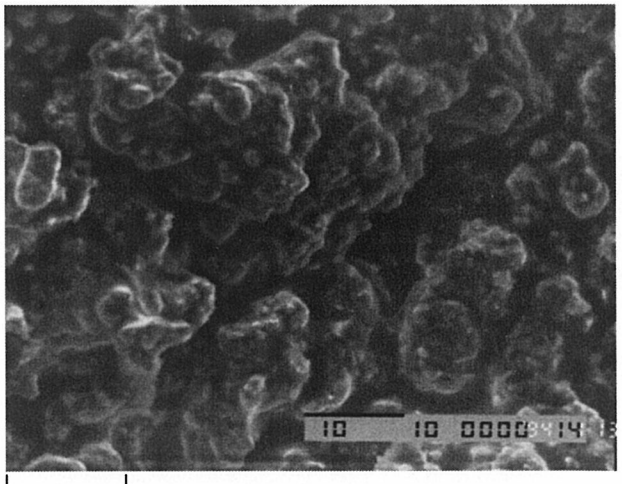

10 μm

(b) L=25mm

Fig. 5 O. Fukumasa

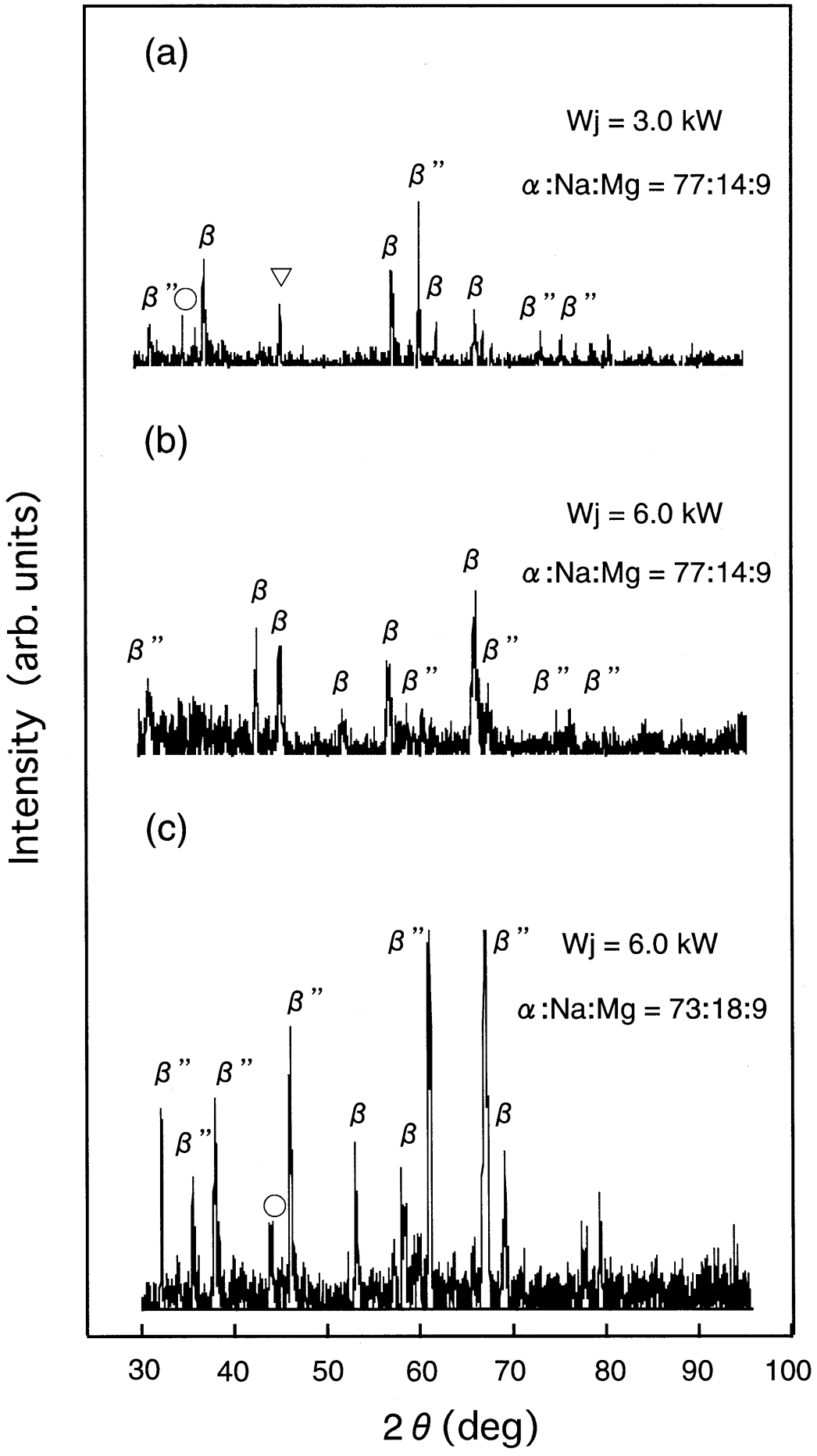

Fig. 6 O. Fukumasa

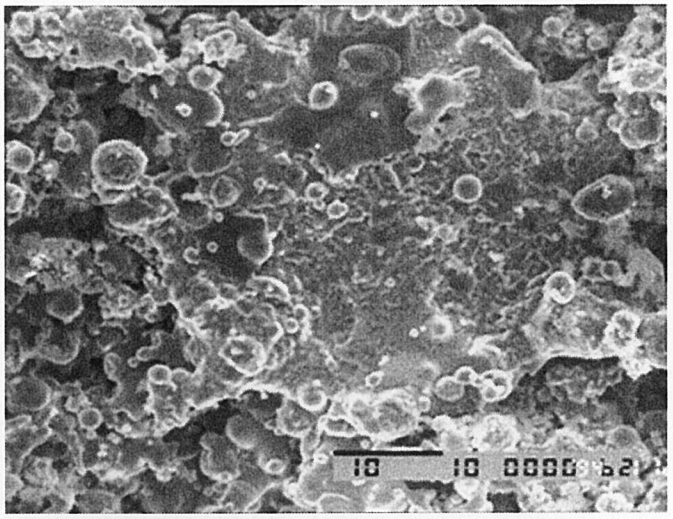

10 μm

(a) Pt = 760Torr

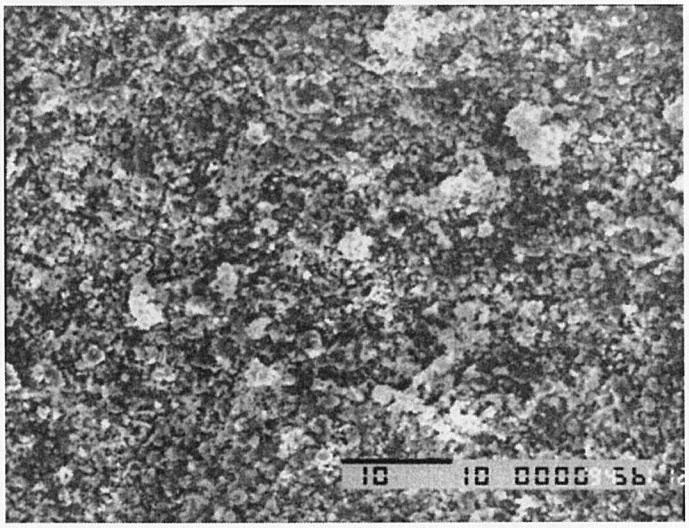

10 μm

(b) Pt = 100Torr

Fig. 7 O. Fukumasa

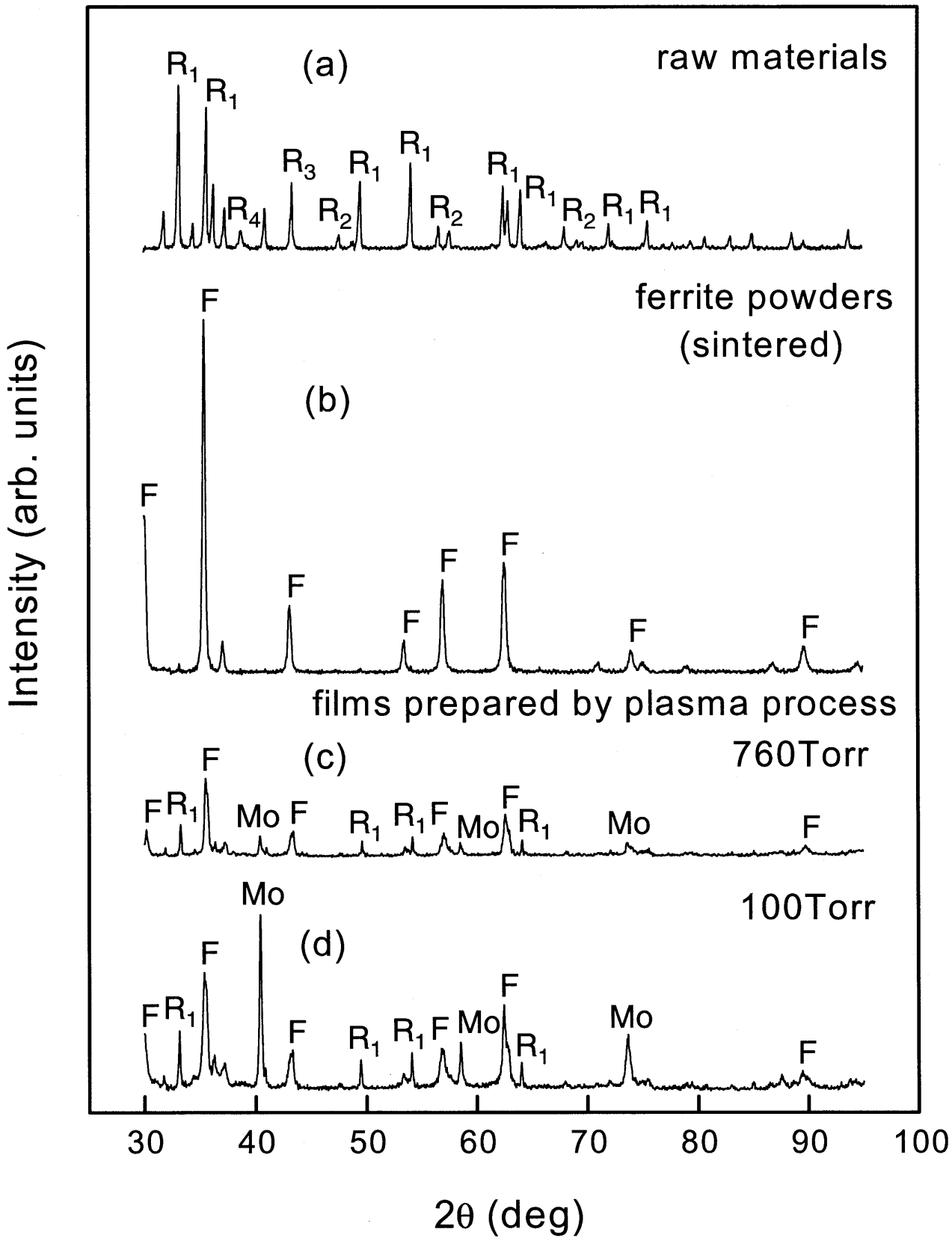

Fig. 8 O. Fukumasa

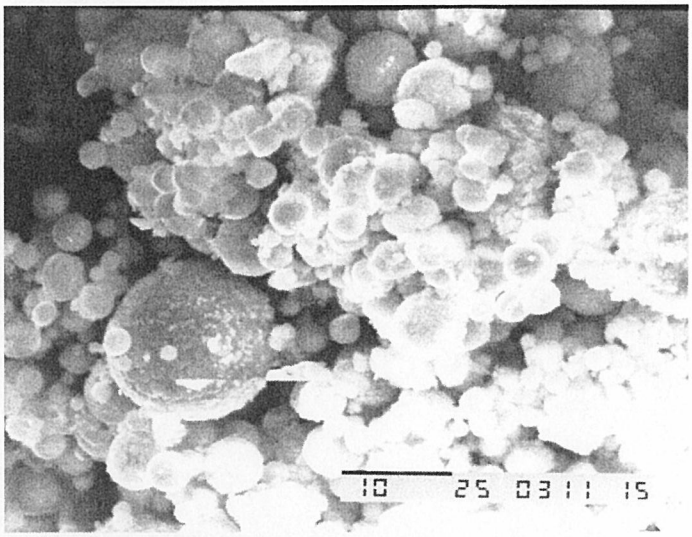

10 μ m

(a) Pt = 760Torr

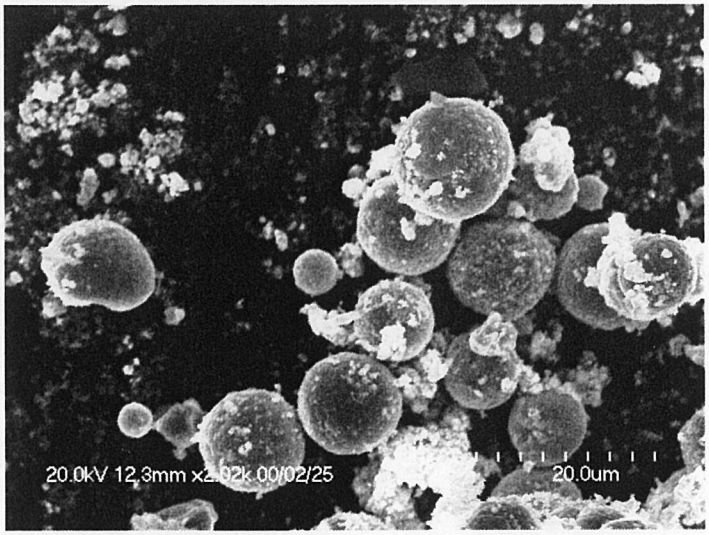

10 μ m

(b) Pt = 100Torr

Fig. 9 O. Fukumasa